

The phenanthridine biguanides efficiently differentiate between dGdC, dAdT and rArU sequences by two independent, sensitive spectroscopic methods.

Marijana Radić Stojković,^a Snežana Miljanić,^b Katarina Mišković,^c Ljubica Glavaš-Obrovac,^{c,d} Ivo Piantanida^{a,*}

Received (in XXX, XXX) Xth XXXXXXXXXX 200X, Accepted Xth XXXXXXXXXX 200X

First published on the web Xth XXXXXXXXXX 200X

DOI: 10.1039/b000000x

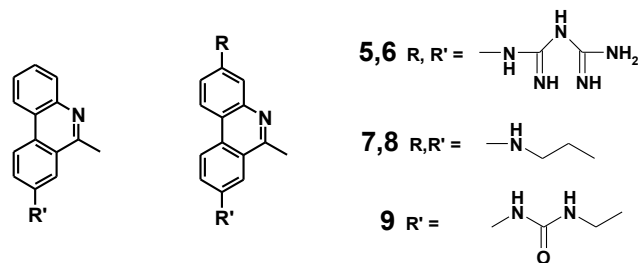
At submicromolar concentrations two novel phenanthridine biguanides exhibit distinctly different spectroscopic signals for dGdC and dAdT sequences, respectively, by opposite fluorimetric changes (quenching for dGdC and increase for dAdT) and especially bis-biguanide derivative gives opposite ICD response (negative ICD for dGC and strong positive for dAdT). This specific signalling was explained by ability of compounds to switch binding mode from intercalation into dGdC to minor groove binding into dAdT sequences. Both compounds bind to rArU by intercalation, yielding different fluorimetric and CD response in comparison to any of aforementioned ds-DNA. Moreover, both compounds revealed significantly higher affinity toward ds-polynucleotides in comparison to previously studied alkylamine- and urea-analogues. Furthermore, DNA/RNA binding properties of novel compounds could be controlled by pH, due to the protonation of heterocyclic nitrogen. Low in vitro cytotoxicity of both compounds against human cell lines makes them interesting spectrophotometric probes.

Introduction

The recognition of specific nucleic acid sequences by novel small molecules has been the subject of a large number of studies over many years.¹ Moreover, small molecules emitting specific or at least highly selective signals upon binding to certain DNA/RNA sequences are important for many technologies used in the molecular biology and medicine.² Small organic molecules can bind to DNA by means of a non-specific (mainly electrostatic) binding along the DNA exterior, a specific groove binding and intercalation which is characterized by insertion of planar aromatic molecules between base pairs and is generally independent of base pair sequence.³

Phenanthridine moiety or its close analogues (e.g. 4,9-diazapyrene) were often applied for an “aryl” component due to characteristic structural features like a permanent or pH induced positive charge, high polarizability, high electron affinity and highly polar amino groups.⁴ In addition, it was shown that the chemical modulation of the phenanthridine exocyclic amines is a profitable option to tune the nucleic acid recognition properties of phenanthridinium dyes.⁵ A lot of experimental data on ethidium derivatives have been collected over the last three decades⁶ including a design of two-colour RNA intercalating probe for cell imaging applications⁷, photoaffinity labelling⁸ and antibiotic as well as antitumor activity.⁹⁻¹² Also, recent study demonstrated that double amine-guanidine substitution at the 3 and 8 positions of the ethidium bromide changed the original intercalator into a minor groove binder of DNA.¹³ Moreover, a single amine-guanidine exchange in known intercalators (anthracene,

pyrene, tiophene, fluorene) resulted in a marked gain of affinity and antiproliferative activity while keeping their intercalative mode of binding.¹⁴ Furthermore, by taking advantage of weakly acidic pK of phenanthridine heterocyclic nitrogen, it was possible to efficiently and reversibly control some interactions with DNA/RNA by external stimuli (pH), as it was previously shown for aliphatic amine – phenanthridine conjugates.¹⁵ In our very recent studies, we noticed that electron-rich substituent as urea attached at 8- position of phenanthridine can induce intriguing fluorimetric specificity against AT (emission increase) and GC (emission quenching) basepairs, which was not previously reported for phenanthridine derivatives.¹⁶ All aforementioned inspired us to design novel phenanthridine derivatives equipped at 3 and/or 8 positions with substituents which can actively participate in non-covalent binding to DNA/RNA, due to steric and electronic properties differentiate between various secondary structures and/or basepair composition of polynucleotide and report that recognition in the spectroscopically feasible form.



Scheme 1. Novel biguanide-phenanthridine conjugates **5** and **6**, and their previously studied aliphatic amine-phenanthridine conjugates **7** and **8**^{17,18} and urea analogue **9**.¹⁶

In a search for promising substituents based on our knowledge on urea,¹⁶ amidine⁵ and guanidine derivatives,⁵ we came across biguanides, whose extended structure in preliminary modelling studies pointed toward intriguing combination of binding and steric interactions. Structural features of such biguanide-phenanthridine conjugates imply interactions between biguanide and DNA/RNA phosphate as well as possible hydrogen bonding of biguanide(s) with nucleobases within one of the DNA/RNA grooves analogously to recently shown guanidiniocarbonyl pyrrole interactions.¹⁹ Moreover, since the early 1900's, biguanides and substituted biguanides containing the active guanidine moiety have proven useful for the treatment of hyperglycemia, malaria and influenza²⁰. Also, biguanide derivatives played important roles in elucidating many interesting aspects of coordination chemistry.²¹ Moreover, biguanides are well known for their antimicrobial,²² antimalarial,²³ antidiabetic²⁴ and antitumor properties.²⁵

Therefore, we decided to study an influence of biguanide substituents attached to the 3 and/or 8 position of the phenanthridine ring (compounds **5**, **6**; Scheme 1) on the binding mechanism of these ligands to DNA/RNA and on their cytotoxic activity. Moreover, to investigate the impact of biguanide- substituents, obtained results are compared with previously studied analogues (Scheme 1) equipped either with inert aliphatic substituents (**7**, **8**) or binding-active urea substituent (**9**). Furthermore, the antiproliferative activity of biguanide-phenanthridine conjugates against tumour cell lines and normal cells was also assayed.

Results and discussion

Synthesis

The most of the arylbiguanides are prepared by the aqueous method of Curd and Rose²⁶ although in several cases pyridine was employed as a solvent. Phenyl 6-methylphenanthridin-8-yl carbamate and diphenyl 6-methylphenanthridine-3,8-diyl dicarbamate were used as the starting material for the synthesis procedure (Scheme 2). Protected phenanthridines were prepared in four steps, starting from the commercially available 2-aminobiphenyl, by the Morgan-Walls reaction²⁷ based on the middle pyridine ring formation by intramolecular electrophilic cyclization of the 2-amidobiphenyl derivative using POCl₃. Removal of phenyloxycarbonyl protection from compounds **1** and **2** was achieved by heating at 120°C under acidic condition. The reaction of aminophenanthridine with 3M hydrochloric acid and dicyandiamide²⁶ afforded compounds **5** and **6** in 59 and 39% yields, respectively.

Spectroscopy

Compounds **5** and **6** due to the biguanide substituents were much better soluble in aqueous solutions (**5**, $c=1.7 \times 10^{-3}$ mol dm⁻³, **6**, $c=1.4 \times 10^{-3}$ mol dm⁻³) than previously studied **8** and **9**. Buffered aqueous solutions of studied compounds were stable for several months. The absorbencies of **5** and **6** (Figure 1) were proportional to their concentrations up to $c=2-2.5 \times 10^{-5}$ mol dm⁻³, changes of the UV/Vis spectra on the temperature increase up to 95°C were negligible and reproducibility of

UV/Vis spectra upon cooling back to 25°C was excellent. All mentioned is indicating that studied compounds do not aggregate by intermolecular stacking at experimental conditions used. Absorption maxima and corresponding molar extinction coefficients (ϵ) are given in Table 1.

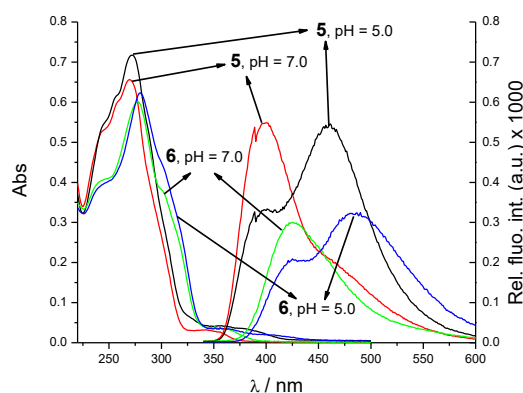
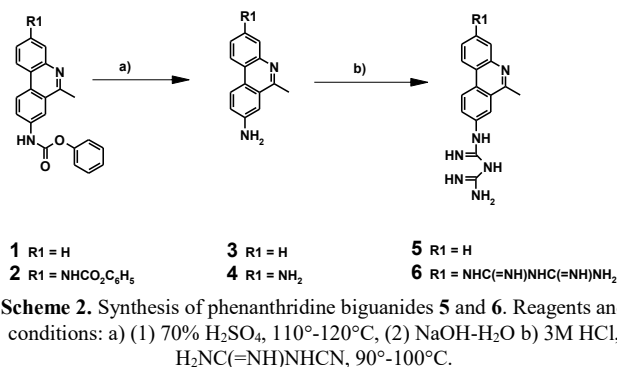


Fig. 1 Left) UV/Vis spectra of **5** and **6** at $c = 2 \times 10^{-5}$ mol dm⁻³; Right) Fluorescence emission spectra of **5** and **6** at $c = 2.8 \times 10^{-6}$ mol dm⁻³; pH 7.0, buffer sodium cacodylate, $I = 0.05$ mol dm⁻³, pH 5.0, citric acid/NaOH buffer, $I = 0.03$ mol dm⁻³.

Table 1 Electronic absorption maxima and corresponding molar extinction coefficients in aqueous medium,^{a,b} fluorescence emission maxima and corresponding relative quantum yields^c.

	UV/Vis		Fluorescence emission, Q^c		
	λ_{\max} (nm) / $\epsilon \times 10^3$ (dm ³ mol ⁻¹ cm ⁻¹)		λ_{\max} (nm)	pH 5.0	pH 7.0
	pH 5.0	pH 7.0			
5	272 / 34.86	270 / 32.61	460 ^a /399 ^b	0.026	0.060
6	280 / 31.68	277 / 30.79	485 ^a /427 ^b	0.017	0.023

^a Buffer pH 5.0 (citric acid/NaOH buffer, $I = 0.03$ mol dm⁻³). ^b Buffer pH 7.0 (buffer sodium cacodylate, $I = 0.05$ mol dm⁻³). ^c Relative quantum yield (Q) was determined with respect to L-N-acetyltryptophanamide (NATA) standard⁵⁹ ($Q = 0.14$).

The emission intensities (Figure 1) of buffered aqueous solutions (buffer sodium cacodylate, $I = 0.05$ mol dm⁻³, pH 7.0, citric acid/NaOH buffer, $I = 0.03$ mol dm⁻³, pH 5.0) of studied compounds are proportional to their concentrations up to $c = 3-4 \times 10^{-6}$ mol dm⁻³, changes of the emission spectra on the temperature increase up to 45°C were only minor at pH 7.0

but somewhat stronger at pH 5.0 and reproducibility of emission spectra upon cooling back to 25°C was excellent. The excitation spectra agree well with corresponding absorption spectra in the region where emission and excitation spectrum do not overlap.

Continuous variation of pH resulted in changes of fluorescence emission intensity of **5** (Figure 2) and **6** characterised by two transition steps, which allowed an estimation of the pK_{a1} value ~ 5.2 and pK_{a2} value ~ 11.3 . In order to obtain more precise pK_a values, potentiometric titration of **5** (data not shown) was performed within pH 3 – 11 range, giving $pK_{a1} = 5.5$ and $pK_{a2} = 10.2$. The first transition step can be attributed to the protonation equilibrium of phenanthridine nitrogen ($pK_a \sim 6$),^{17,18} with well separated protonated ($\lambda_{max} = 462$ nm) and non-protonated nitrogen species ($\lambda_{max} = 399$ nm), whereas latter transition step can be attributed to the protonation equilibrium of biguanide moiety.²⁸ Consequently, at acidic pH (pH 5.0, citric acid/NaOH buffer, $I = 0.03$ mol dm⁻³) phenanthridine nitrogen of **5** and **6** is mostly protonated (76%), consequently **5** is characterized by two positive charges and **6** (with two biguanide groups) has three positive charges. On the other hand, at neutral conditions (pH 7.0, buffer sodium cacodylate, $I = 0.05$ mol dm⁻³) phenanthridines of **5** and **6** are not protonated and compounds are characterized by one or two positively charged biguanides, respectively.

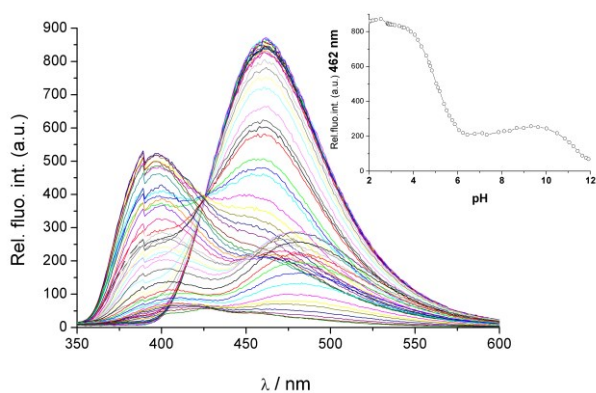


Fig. 2 The pH dependent changes of fluorescence emission spectrum of **5** ($c = 2.0 \times 10^{-6}$ mol dm⁻³); $\lambda_{exc} = 272$ nm (left); Dependence of **5** fluorescence intensity at $\lambda_{max} = 462$ nm on the pH of the aqueous solution (right).

Study of interactions of **5** and **6** with ds- DNA and ds-RNA in aqueous medium

Spectrophotometric titrations

In all titration experiments, equilibrium was achieved within 2 min upon mixing DNA or RNA with studied compound. Such kinetics of binding is common for small molecules, both for intercalators (e.g. ethidium bromide) and minor groove binders (e.g. DAPI or related derivatives), thus ruling out some secondary processes like degradation of compounds upon DNA/RNA binding or formation of more complicated complexes like threading intercalation or self-stacking agglomerates of porphyrins.

UV/Vis titrations were not applicable for study of interactions

of **5** and **6** with ds-DNA and RNA due to their low molar extinction coefficients at $\lambda > 300$ nm. Nevertheless, strong fluorescence emission of the **5** and **6** aqueous solutions allowed titration studies. At both pH, all studied compounds showed similar fluorimetric changes toward ds-DNA and ds-RNA. However, fluorescence changes were strongly dependent on a structure of the polynucleotide, whereby addition of dAdT polynucleotide (at excess of a polynucleotide, Figure 3, Up) resulted in emission increase of **5** and **6**, while titration with dGdC polynucleotide (Figure 3, Down) yielded strong fluorescence quenching for both compounds.

Such a specific fluorimetric differentiation between AT and GC sequences was not common for phenanthridine moiety, whose fluorescence is either non-selectively enhanced (ethidium bromide analogues) or completely quenched (derivatives with no amino-substituents at 3,8 positions).⁴⁻⁵ Actually very few compounds reveal such emission specificity (some 4,9-diazapyrenium cations²⁹ and acridine derivatives³⁰) and only very recently urea-phenanthridine conjugate (e.g. compound **9**, Scheme 1).¹⁶ That dAdT vs dGdC fluorescence specificity was correlated to intercalation of mentioned compounds into ds-DNA, whereby only aromatic stacking interactions with guanine base yielded quenching (due to the electronic property of guanine, being the most electron-donating of all four nucleobases).^{30,31}

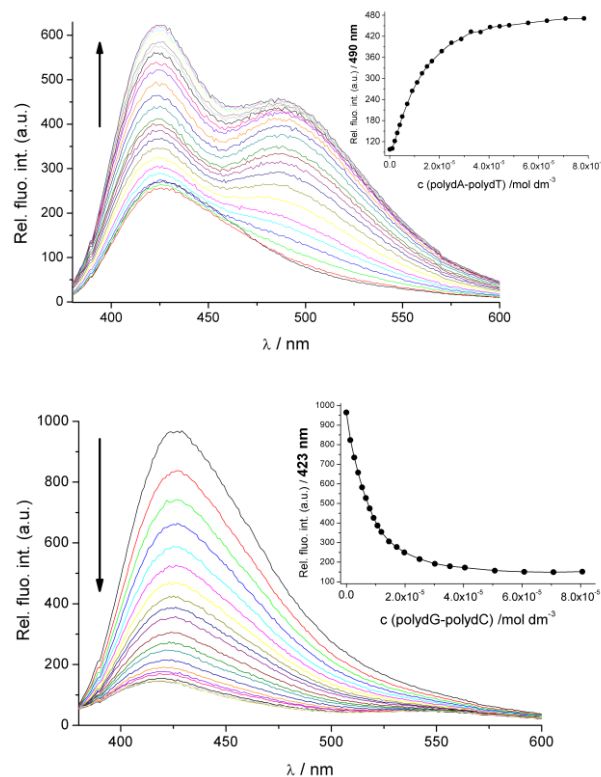


Fig. 3 Up) Changes of fluorescence spectrum of **6** ($c = 1.0 \times 10^{-6}$ mol dm⁻³) upon titration with poly dA – poly dT; Down) Changes in fluorescence spectrum of **6** ($c = 1.3 \times 10^{-6}$ mol dm⁻³) upon titration with poly dG – poly dC; Done at pH 7.0, buffer sodium cacodylate, $I = 0.05$ mol dm⁻³.

However, fluorimetric changes of **5** and **6** upon addition of ds-

RNA (poly rA-poly rU) revealed different pattern in comparison to DNA polynucleotides. Namely, at pH 7.0 poly rA-poly rU induced fluorescence quenching of **5** at maximum ($\lambda_{em} = 400$ nm, which is assigned to non-protonated phenanthridine nitrogen form according to Figure 2), while at the other maximum (463 nm) it increased fluorescence of **5** (Figure 4). Such a change along with systematic deviation from isosbestic point (420-430 nm) indicates formation of two different **5**-poly rA – poly rU complexes. At 463 nm maximum, a few first aliquots of poly rA – poly rU yielded a minor quenching of **5** fluorescence until ratio $r = [5] / [\text{poly rA} - \text{poly rU}] = 0.042$ and further addition of poly rA – poly rU yielded significant fluorescence increase. Similar dual fluorimetric responses but with emphasis on the increase of **6** fluorescence at one maximum wavelength ($\lambda_{em} = 485$ nm, which is ascribed to protonated phenanthridine nitrogen form analogously to **5** in Figure 2) were observable in titrations with poly rA – poly rU at pH 5.0 and pH 7.0. Such mixed binding modes of **5** and **6** to poly rA – poly rU could not be resolved according to the fluorimetric titrations only, but other independent methods were necessary.

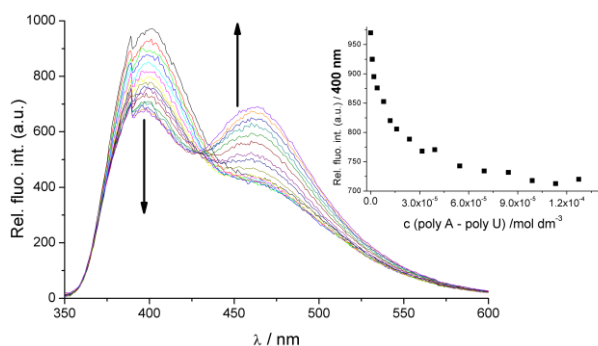


Fig. 4 Changes in fluorescence spectrum of **5** ($c = 1.0 \times 10^{-6}$ mol dm⁻³) upon titration with poly rA – poly rU; at pH 7.0, buffer sodium cacodylate, $I = 0.05$ mol dm⁻³.

Processing of the fluorescence titration data collected at excess of polynucleotide over compound by means of Scatchard equation³² gave binding constants K_s and ratios $n_{[\text{bound compound}]/[\text{polynucleotide}]}$ (Table 2). In case of **5** with poly rA – poly rU, titration data of both fluorescence quenching and increases were separately processed by means of Scatchard equation. At neutral conditions, **5** revealed somewhat stronger affinity toward poly rA – poly rU and poly dA – poly dT compared to poly dG – poly dC.

The most importantly, previously studied aliphatic analogues **7** and **8** as well as urea-analogue **9** (Scheme 1) revealed 10-100 times lower affinity toward corresponding DNA and RNA

than here presented **5** and **6**, which clearly points to significant contribution of biguanide substituents in DNA/RNA binding.

Table 2 Binding constants ($\log K_s$)^a and ratios n^b ([bound compound]/[polynucleotide phosphate]) calculated from the fluorescence titrations of **5** and **6** with ds- polynucleotides at pH 5.0 (citric acid/NaOH buffer, $I = 0.03$ mol dm⁻³) and pH 7.0 (buffer sodium cacodylate, $I = 0.05$ mol dm⁻³)

		5			6		
		I/I_0^c	$\log K_s$	n	I/I_0^c	$\log K_s$	n
pH 5	poly rA - poly rU	3.05	6.96	0.098	5.47	7.36	0.15
	poly dA- poly dT	2.36	6.98	0.04	4.24	7.4	0.089
	poly dG - poly dC	0	6.81	0.05	0	6.63	0.105
pH 7	poly rA - poly rU	0.76 ^d 1.9 ^e	5.96 7.53	0.1 0.01	10.1	5.73	0.33
	poly dA- poly dT	1.76	7.59	0.007	5.84	6.52	0.071
	poly dG - poly dC	0.4	5.56	0.6	0	5.80	0.29

^a Titration data were processed according to the Scatchard equation;³² ^b Accuracy of $n \pm 10 - 30\%$, consequently $\log K_s$ values vary in the same order of magnitude ^c I_0 – starting fluorescence intensity of **5** and **6**; I – fluorescence intensity of **5**, **6** /polynucleotide complex calculated by Scatchard equation. ^d Data calculated by the Scatchard equation from the part of titration experiment ($\lambda_{max} = 400$ nm) with poly rA – poly rU in which starting fluorescence of **5** was quenched. ^e Data calculated by the Scatchard equation from the part of titration experiment ($\lambda_{max} = 463$ nm) with poly rA – poly rU in which fluorescence of primarily formed complex **5**-poly A-polyU was enhanced by formation of secondary complex.

Circular dichroism experiments

So far, non-covalent interactions at 25°C were studied by monitoring the spectroscopic properties of studied compound upon addition of the polynucleotides. The CD spectra of the ligand-polynucleotide complexes can provide information on two levels.³³ First, the conformation change of polynucleotide upon small molecule binding can be probed through the changes of the intrinsic polynucleotide CD spectrum. Second, achiral small molecules could acquire an induced CD (ICD) signal when they form complexes with a polynucleotide from which a mutual orientation of small molecule and polynucleotide chiral axis could be derived, consequently giving an useful information about modes of interaction.^{34,35} It should be noted that here studied compounds **5** and **6** are achiral and therefore do not possess intrinsic CD spectrum. Since studied compounds display the UV/Vis spectra in the 245 – 350 nm region (Figure 1), the ICD bands observed at $\lambda > 300$ nm can be attributed to them.

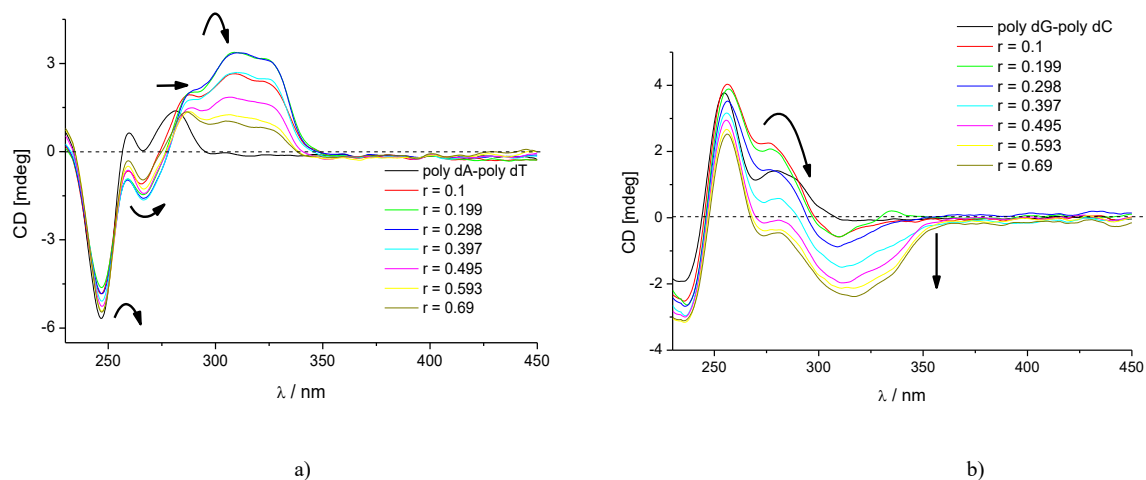


Fig. 5 CD titrations of a) poly dA – poly dT and b) poly dG-poly dC ($c = 3.0 \times 10^{-5} \text{ mol dm}^{-3}$) with **6** at molar ratios $r = [\text{compound}] / [\text{polynucleotide}]$ (pH 5.0, citric acid/NaOH buffer, $l = 0.03 \text{ mol dm}^{-3}$).

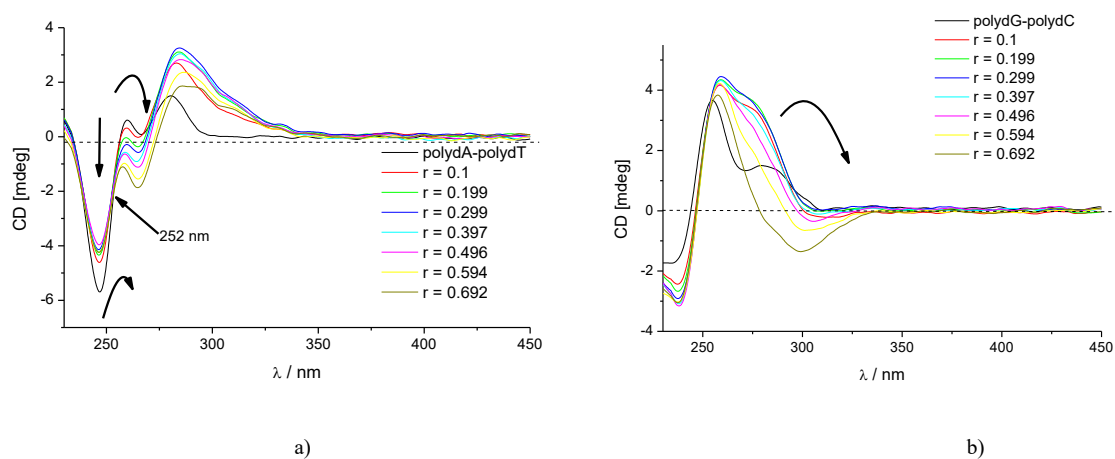


Fig. 6 CD titrations of a) poly dA – poly dT and b) poly dG-poly dC ($c = 3.0 \times 10^{-5} \text{ mol dm}^{-3}$) with **5** at molar ratios $r = [\text{compound}] / [\text{polynucleotide}]$ (pH 5.0, citric acid/NaOH buffer, $l = 0.03 \text{ mol dm}^{-3}$).

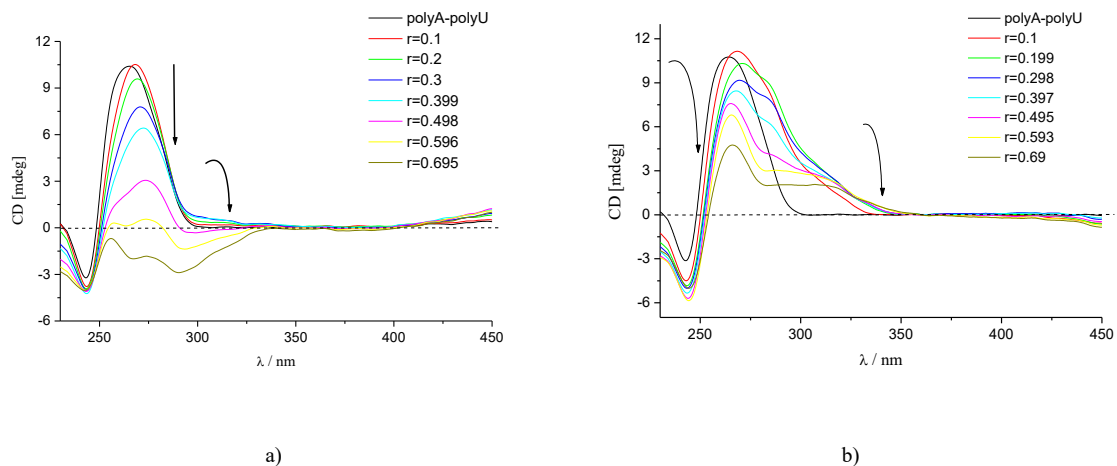


Fig. 7 CD titration of poly rA-poly rU ($c = 3.0 \times 10^{-5} \text{ mol dm}^{-3}$) with **5** (a) and **6** (b) at molar ratios $r = [\text{compound}] / [\text{poly rA-poly rU}]$ (pH = 5.0, citric acid/NaOH buffer, $l = 0.03 \text{ mol dm}^{-3}$).

In general, changes in CD spectra of studied polynucleotides obtained upon mixing with **5** and **6** were dependent on a pH of the solution, whereby protonation of the heterocyclic nitrogen of **5**, **6** resulted in stronger changes in the CD spectra of ds-DNA and RNA at pH 5.0 (Figures 5 and 6).

In the most CD experiments the ICD signals for both **5** and **6** differed at ratio $r_{[\text{dye}]/[\text{polynucleotide}]} < 0.2$ and $r \gg 0.2$. For both, intercalative and minor groove binding mode, at ratios below $r < 0.2$ there is an excess of binding sites over concentration of **5** or **6**, thus allowing each of small molecules to bind to its own binding site – consequently observed ICD bands can be attributed to one dominant binding mode. However, when all dominant binding sites filled (at ratios $r \gg 0.2$, excess of **5** or **6** over the binding sites), excess of small molecules still tends to bind to polynucleotide, by forming aggregates along double helix. For instance, at such conditions even ethidium bromide and many other intercalators bind by non-intercalative binding mode, and many minor groove binders tend to form dimers within the grooves (e.g. cyanine dyes).³⁵

At both pH 5.0 and pH 7.0, additions of **5** and **6** into AT-polynucleotide solutions resulted in very strong positive ICD bands within the 290-350 nm range, which is indicative of minor groove binding to the AT sites.³⁶ A clear isoelliptic point at 252 nm for ratio $r = 0 - 0.3$ (Figure 5 and Figure 6) pointed toward formation of one dominant type of **5,6**/polynucleotide complex.

A completely different pattern was observed in CD experiments of dGdC polynucleotides with **5** and **6**. The weak negative ICD band at $\lambda > 290$ nm obtained at low ratios $r_{[\text{5,6}]/[\text{dGdC}]} = 0 - 0.2$ for both, **5** and **6** (Figures 5 and 6), which reflects an orientation of the phenanthridine chromophore more or less coplanar to the plane of polynucleotide basepairs could be attributed to intercalation between basepairs.³⁷ However, at conditions of an excess of **5**, **6** over intercalative binding sites ($r_{[\text{5,6}]/[\text{dGdC}]} > 0.2$) stronger negative ICD bands appear accompanied by systematic deviation from the isoelliptic points, which suggests agglomeration of **5**, **6** along DNA.

Addition of **6** induced changes in CD spectra of ctDNA (composition 58% AT, 42% GC) similar to those with AT-polynucleotides (the increase of CD spectra in the 260-290 region and strong positive ICD at $\lambda > 290$ nm) at both, pH 5.0 and pH 7.0. Contrary to **6**, no positive ICD band at $\lambda > 290$ nm was observed for ctDNA-**5** complex at both pH which could be the consequence of mixed binding modes, e.g. minor groove binding in AT rich sequences and intercalation into GC-rich sequences.

Similarly to fluorimetric titrations, CD experiments with poly rA- poly rU (Figure 7) differed significantly from analogous AT-DNAs (Figures 5a, 6a), whereby intensity of CD spectrum of poly rA - poly rU strongly decreased and intensity of CD spectrum of poly dA – poly dT increased. Moreover, strong positive ICD bands at $\lambda > 290$ nm obtained for AT-DNAs contrasted very weak positive or even negative ICD bands at $\lambda > 290$ nm observed for poly rA - poly rU. Another prominent difference was evidenced at pH 7 (ESI†), at which CD spectra of poly rA - poly rU changed only negligibly, at variance to

moderate to strong changes in CD spectra of AT-DNAs.

Absence of strong positive ICD band at $\lambda > 290$ nm excludes binding of **5**, **6** into minor groove of ds-RNA, which is anyway too broad and shallow³⁹ to efficiently bind such small molecules.³ However, a weak positive ICD band ($\lambda > 290$ nm) observed at ratios $r_{[\text{5,6}]/[\text{poly rA - poly rU}]} < 0.3$ can be attributed to intercalation of **5**, **6** into poly rA - poly rU, whereby positive sign implies orthogonal orientation of the longer axis of phenanthridine in respect to the longer axis of adjacent basepairs.³⁵ Intriguingly, almost the same changes in CD spectrum of poly A- poly rU were observed for urea-analogue **9**¹⁶ (ESI†), a proven RNA intercalator. The most prominent changes in CD spectra in the range 260 – 300 nm observed at the excess of **5**, **6** over the intercalation binding sites ($r \gg 0.3$), can be attributed to the non-specific agglomeration of non-intercalated molecules along double helix.^{34,35}

Thermal denaturation experiments

The melting temperature (T_m) is defined as the temperature at which half of the DNA strands are in the double-helical state and half are in the "random-coil" states. It depends on both the length of the molecule and the specific nucleotide sequence composition of that molecule. It can also be influenced by salt concentration and pH. Non-covalent binding of small molecules to ds-polynucleotides usually has certain effect on the thermal stability of helices thus giving different T_m values. Difference between T_m value of free polynucleotide and complex with small molecule (ΔT_m value) is important factor in characterisation of small molecule / ds-polynucleotide interactions.³⁸

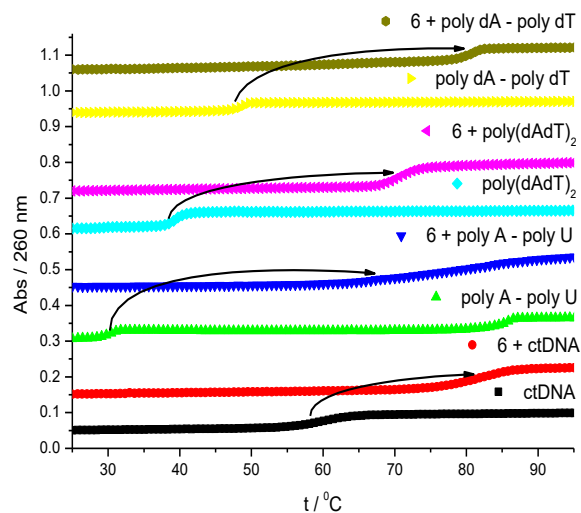


Fig. 8 Thermal denaturation of studied polynucleotides upon addition of **6**. Ratio $r_{[\text{6}]/[\text{polynucleotide}]} = 0.3$, pH 5.0 (citric acid/NaOH buffer, $I = 0.03 \text{ mol dm}^{-3}$).

At both, pH 5 and 7, for all studied polynucleotides, thermal stabilization effects (Table 3, Figure 8). were proportional to the number of positive charges attached to the phenanthridine moiety, consequently the highest ΔT_m values were obtained for **6** (2+ at pH 7, 3+ at pH 5), somewhat lower for **5** (1+ at pH 7, 2+ at pH 5) and significantly lower for

previously studied aliphatic analogues **7** and **8** as well as urea-analogue **9** (neutral at pH 7, 1+ at pH 5), which again clearly points to significant contribution of biguanide substituents in DNA/RNA binding.

More detailed examination of results at pH 5 revealed that stabilization effects observed for AT and rArU polynucleotides were comparable (for each compound alone) and for mixed sequence (ct-DNA, 58% AT, 42% GC)

somewhat lower.

Intriguingly, at pH 7 only bis-biguanide derivative **6** significantly stabilized all studied polynucleotides, whereby AT-sequences were significantly stronger stabilized than AU- or mixed (ct-DNA) sequence. Mono-biguanide derivative **5** stabilized weakly only alternating AT-sequence.

Table 3 The $^a\Delta T_m$ values (°C) of studied ds- polynucleotides upon addition of different ratios $^b r$ of **5** and **6** at pH 5.0 (citric acid/NaOH buffer, $I = 0.03 \text{ mol dm}^{-3}$) and pH 7.0 (buffer sodium cacodylate, $I = 0.05 \text{ mol dm}^{-3}$).

	5			6			8¹⁷	9¹⁶	
	0.1	0.2	0.3	0.1	0.2	0.3	0.3	0.3	
pH 5	ctDNA	6.6	8.7	10.4	14.5	20.6	22.3	-	2.4
	poly dA-poly dT	6.7	9.3	11.4	26.3	29.5	32.2	13.0	0.7
	poly rA - poly rU	12.2/ 0 ^c	15/ -0.5 ^c	16.7/ -0.5 ^c	35.1/ -0.7 ^c	35.4/ -1.8 ^c	36.5/ -2.1 ^c	7.9/ 0 ^c	3.4/ 0 ^c
	poly dAdT - poly dAdT	10.6	13.7	16.2	21.8	25	30	2.0	-
pH 7	ctDNA	0	0	0	3.7	5.6	7.3	-	-
	poly dA-poly dT	0.3	0.4	0.5	7.2	9.8	11.7	-	-
	poly rA - poly rU	0	0	0	3.5	5.0	6.5	-	-
	poly dAdT - poly dAdT	1.2	1.9	2.5	7.0	10.3	12.1	-	-

^a Error in ΔT_m : $\pm 0.5^\circ\text{C}$; ^b $r = [\text{compound}] / [\text{polynucleotide}]$; ^c Biphasic transitions: the first transition at $T_m = 30.5^\circ\text{C}$ is attributed to denaturation of poly rA – poly rU and the second transition at $T_m = 85.9^\circ\text{C}$ is attributed to denaturation of poly AH⁺-poly AH⁺ since poly rA at pH 5.0 is mostly protonated and forms ds-polynucleotide³⁹.

Viscometry measurements

The increase in ds-DNA/RNA contour length, which should happen upon intercalation of aromatic moiety, is conveniently monitored by measuring the viscosity of sonicated rodlike fragments of ds-DNA/RNA as a function of ligand binding ratio, $r_{[\text{compound}] / [\text{polynucleotide}]}$. Cohen and Eisenberg have deduced that the relative increase in contour length in the presence of bound drug is approximated by the cube root of the ratio of the intrinsic viscosity of the DNA-drug complex to that of the free DNA (equation in Materials and Methods).⁴⁰ Classical monointercalators like ethidium bromide, proflavine and 9-aminoacridine have values of helix extension parameter (viscosity index), α of about 0.8-0.9 while extension parameters of bisintercalators are usually in the range 1.5-1.9.⁴⁰ Complexes and ligands that bind exclusively or at least partially in the DNA grooves typically cause less pronounced or no changes in DNA/RNA solution viscosity.

Viscometry experiments (ESI[†]) were performed with ct-DNA and poly rA – poly rU at pH 7.0 (buffer sodium cacodylate, $I = 0.05 \text{ mol dm}^{-3}$). The values of helix extension parameter for poly rA – poly rU were $\alpha = 0.77 \pm 0.05$ (**5**), 0.91 ± 0.06 (**6**), latter value agreeing well with the value obtained for ethidium bromide ($\alpha(\text{EB}) = 1.02 \pm 0.08$). Those results strongly support

intercalation of **6** into poly rA – poly rU as the dominant binding mode, while α value obtained for **5** suggested mixed binding mode or agglomeration along RNA double helix. For ct-DNA values of $\alpha = 0.62 \pm 0.06$ (**5**), 0.31 ± 0.03 (**6**) are only half of the value found for **EB** ($\alpha = 1.04 \pm 0.09$). Since ct-DNA consists of mixed sequence (42% GC basepairs/58%AT basepairs), obtained α values suggest intercalation of **5**, **6** in the GC-rich sequences resulting in significant DNA elongation (e.g. $\alpha \sim 1$) and minor groove binding in AT rich domains, which should have only minor impact on DNA elongation due to the stiffening of double helical structure – thus overall ctDNA elongation should be about $\alpha = 0.4-0.5$. That presumption is additionally supported by experiments performed with dGdC and dAdT polynucleotides (ESI[†]), whereby ratio $\alpha_s/\alpha_{\text{EB}} = 0.8 \pm 0.14$ clearly points that **5** elongates dGdC sequence similarly to ethidium bromide, while ratio $\alpha_s/\alpha_{\text{EB}} = 0.48 \pm 0.11$ is much lower and therefore excluded intercalation as a dominant binding mode.⁵²

Surface-enhanced Raman spectroscopy

Surface-enhanced Raman spectroscopy (SERS) has been used as a powerful technique to study small molecules and their interactions with certain targets such as nucleic acids and intracellular enzymes.⁴¹⁻⁴⁶ When adsorbed on the metal

surface fluorescence of the drug molecules is quenched, at the same time Raman scattering being enhanced by several orders of magnitude. A large amount of a biological sample usually required for conventional Raman measurements (10^{-2} M) is avoided preserving information on structural features of species at concentrations as low as 10^{-8} M. During adsorption of the drug/DNA complex on the surface of the silver nanoparticles neither perturbations of the molecular interactions nor changes in the structure of complexes have been obtained.^{42,43}

Surface-enhanced Raman spectra of the phenanthridine biguanides **5** and **6** and their complexes with ct-DNA were measured in the silver citrate colloid (Figures 9 and 10). A tentative assignment of the observed vibrational bands is given in ESI† (Table S1). The bands are mainly assigned to the stretching and deformation modes of the phenanthridine moiety and CN bonds as well as to bending of amino groups in the biguanide substituents.⁴⁷⁻⁵⁰ In agreement with the vibrational analysis of inorganic and organic salts of biguanide, one band often arises from a mixed vibration involving different functional groups.^{49,50}

Since the buffered solution of the nucleic acid (pH 7.0) was used for preparation of the **5,6**/DNA mixtures, influence of the cacodylate buffer on the **5,6** SERS spectra was examined first. The SERS spectrum of **5** in the presence of the buffer solution is almost identical to its SERS spectrum without the buffer. For **6**, however, intensity of the band at 1426 cm^{-1} associated with CN stretching and NH_2 bending decreased. Slight enhancement of the bands in the region below 1000 cm^{-1} in the spectra of both compounds implies mild aggregation of the silver nanoparticles, most likely induced by the chloride ions present in the buffer solution.

Upon addition of ct-DNA in the silver colloids containing biguanide species (**5,6**/[DNA] 1/20) the Raman scattering was less enhanced than that observed in the colloids containing **5** and **6** alone (Figures 9 and 10). Due to a short range character of the Raman enhancement it can be assumed that interacting with the nucleic acid, biguanide molecules either change their orientation relative to the metal nanoparticles to the position where polarizability change contributes to a lesser degree to the scattering or move away from the enhancing surface. Moreover, a band at 227 cm^{-1} assigned to the Ag–N stretching in the phenanthridine biguanides spectra, shifts towards 224 and 223 cm^{-1} in the SERS spectra of **5**/DNA and **6**/DNA, respectively. The observed downshift indicates weakening of the bond between the phenanthridine biguanides and the silver surface in the presence of DNA.

A shoulder at 1616 cm^{-1} in the spectrum of **5**, which is attributed to the stretching of the double CN bond, turns into a band at 1612 cm^{-1} in the spectrum of **5**/DNA (Figure 9). A shift towards lower wave numbers is also observed for bands at 1422 , 1229 and 1007 cm^{-1} which are assigned to coupling of the CN stretching and NH bending modes. It can be assumed that due to interactions with DNA, electrons are drawn from the C=N bond that lowers the bond order and hence the frequency of the C=N stretching.⁵¹ In the same way CN bonds weaken, resulting in lower vibration energies.

However, some vibrational bands of **5**, such as those at 1210 , 1076 and 588 cm^{-1} , are upshifted in the presence of DNA and appear at 1212 , 1081 and 600 cm^{-1} in the spectrum of the complex. These weak bands are associated predominantly with the NH bending mode. It is very likely that deformation motions of the amino groups are “stiffened” by hydrogen bonding with the nucleic acid, requiring higher energy for vibration.⁵¹ Wavenumbers of the intense bands assigned to the stretchings of the phenanthridine moiety do not significantly change in the spectrum of the complex, however, their intensities relative one to another do. Thus the ratio of the Raman intensity of the bands at 1345 and 1391 cm^{-1} , which is 1.30 for **5** alone, decreases to the value of 1.15 in the spectrum of **5**/DNA. The obtained change in the relative band intensity indicates that due to interaction with DNA the phenanthridine plane adopt tilted position relative to the silver surface giving rise to differently enhanced ring modes.

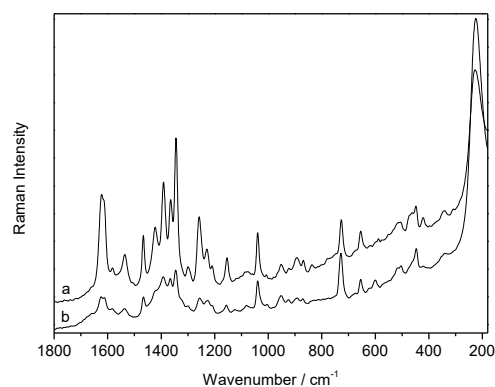


Fig. 9 SERS spectra of a) **5** and b) **5**/[ctDNA] 1/20. $c(\mathbf{5}) = 5 \times 10^{-5}$ M, pH 7.0, buffer sodium cacodylate, $I = 0.05\text{ mol dm}^{-3}$.

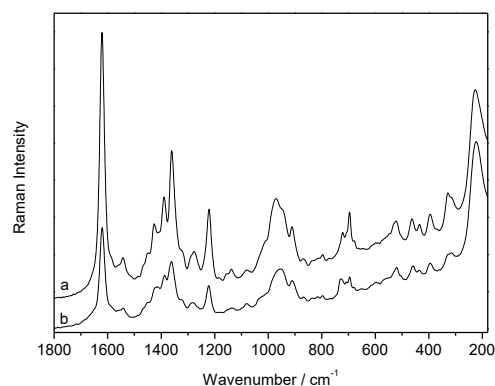


Fig. 10 SERS spectra of a) **6** and b) **6**/[ctDNA] 1/20. $c(\mathbf{6}) = 5 \times 10^{-5}$ M, pH 7.0, buffer sodium cacodylate, $I = 0.05\text{ mol dm}^{-3}$.

Changes in the SERS spectrum of the compound **6** having two biguanide moieties in interaction with DNA resemble those observed in the spectrum of **5**/DNA (Figure 9). Intensity of a band at 1426 cm^{-1} assigned mainly to the CN stretching decreases, forming a shoulder at 1419 cm^{-1} in the spectrum of

the **6**/DNA complex. On the other hand, a medium band at 1277 cm⁻¹, which beside the in plane CH deformations corresponds to the NH bending, shifts towards a higher wavenumber, 1284 cm⁻¹. Unlike the spectrum of **5**/DNA, stretching of the double CN bond contributes along with the phenanthridine stretching vibrations to a very intense band at 1621 cm⁻¹. Except from intensity decrease, a prominent change neither in shape nor in position was obtained for this strong band in the presence of DNA.

In the spectra of both, **5**/DNA and **6**/DNA, bands that originate from ring deformation at 727 and 722 cm⁻¹, respectively, appear at 729 cm⁻¹. Upward shift implies hindered bending of the phenanthridine part upon interaction with the nucleic acid. As for **5**, the relative intensity of the ring modes changes, most likely as a consequence of the interaction induced change in position of the bound molecules of **6** close to the enhancing surface.

In conclusion, quenching of the SERS intensity has been already interpreted as a loss of accessibility for DNA-bound ligands to the silver nanoparticles as a result of a drug binding into ds-DNA, by intercalation and/or minor groove binding.⁴¹⁻⁴⁴ Here, still remaining residual SERS signal indicates that both phenanthridine biguanides upon binding to the DNA helix still remain in contact with silver nanoparticles, although somewhat tilted in respect to the metal surface – that observation agrees much better with DNA minor groove binding than intercalation. In addition, more pronounced spectral changes for **5** than for **6** complex with ctDNA, if compared with the free biguanide molecules point to deeper and more tight insertion of bis-biguanide derivative (**6**), agreeing well with results of CD and especially thermal denaturation experiments.

Discussion of the results of DNA/RNA binding studies

The fluorimetric and CD titrations, thermal denaturation and viscometry experiments clearly indicate for **5** and **6** two different binding modes to ds-DNA's: 1) minor groove binding within dAdT-sequences and 2) intercalation into dGdC-sequences.⁵² Moreover, shifting of some vibrational bands (predominantly associated with the NH bending mode) of **5** and **6** in the presence of ct-DNA also supported deeper and more tight insertion of bis-biguanide derivative (**6**) in comparison to mono-biguanide **5**, agreeing well with results of CD and especially thermal denaturation experiments (only compound **6** stabilizes ct-DNA at pH 7).

The data obtained at pH 5 for **5** and **6** at ratios $I_{[5, 6]}/[poly\ rA - poly\ rU] < 0.3$ point to the intercalation into poly rA – poly rU.⁵² However, at pH 7 mono-biguanide **5** did not stabilize ds-RNA against thermal denaturation and yielded intriguing specific dual fluorimetric response suggesting at least two different binding modes. Quenching of the fluorescence at 400 nm is probably the result of agglomeration of **5** molecules along the polynucleotide backbone, which is consistent with the observed minor changes of CD spectra of poly rA – poly rU at pH 7.0. At variance to **5**, bis-biguanide **6** clearly stabilizes ds-RNA even at pH 7, whereby CD titration and viscometry results support intercalation as a dominant binding mode.

Finally, affinity of **5** and **6** toward all studied DNA/RNA, as well as thermal stabilisation effects are one-two orders of

magnitude higher than those found for previously studied aliphatic analogues **7** and **8** as well as urea-analogue **9**, which clearly points to the significant contribution of biguanide substituents in DNA/RNA binding.

Antiproliferative activity of **5** and **6** and discussion of **5,6** bioactivity

Since **5** and **6** revealed significant interactions with ds-DNA, we evaluated their *in vitro* cytotoxic activity by the MTT assay on a panel of eight human cell lines, six of which were derived from different cancer types including HeLa (cervical carcinoma), MCF-7 (breast carcinoma), AGS (gastric adenocarcinoma), MiaPaCa-2 (pancreatic carcinoma), HEp-2 (laryngeal carcinoma), NCI-H358 (bronchioalveolar carcinoma), one from normal human fibroblasts, BJ, and one from canine Cocker Spaniel kidney, MDCK. Applied in concentration range 10⁻⁷ to 10⁻⁵ mol dm⁻³ compounds did not inhibited the growth of tumour and normal cells. According to the obtained results, antiproliferative activity of **5** was concentration and cell line dependent (ESI[†]). Compared to the inhibitory potential of compound **6**, 0.1 mol dm⁻³ compound **5** exhibited significant antiproliferative activity (Table 4). The significant influence of **5** on tumour cells growth compared to normal cells was not observed instead of different cell metabolism of tumour cells vs. normal cells⁵³. As expected, the pancreatic adenocarcinoma cells, which are extremely resistant to conventional therapy⁵⁴, were most resistant against applied compounds. There are several factors that could explain a difference in growth inhibitory effects between two phenanthridine biguanides: smaller molecular weight of compound **5**, one positive charge on the long axis of the **5** molecules and amphiphilic nature of **5**. All that factors can facilitate drug uptake across the tumour cell membrane which is greatly influenced by the interstitial and intracellular pH and the ionization properties of the drug⁵⁵. Thus, the obtained data demonstrated how minor changes to the structure of these compounds can significantly influence on the final outcome in antitumor activity resulting in either significant antitumor activity in higher applied concentration (as for **5**) or almost complete loss of antitumor activity (in case of **6**).

Table 4 IC₅₀ – Compound concentration (μmol dm⁻³) leading to cellular viability reduction by 50% compared to control cells after 72 h treatment. Data represent mean value of three independent experiments ± SD. Cytotoxic activity was analyzed by MTT assay.

	IC ₅₀ (μmol dm ⁻³)							
	AGS	MiaPaCa2	CaCo-2	HEp-2	HeLa	NCI-H358	BJ	MDCK
5	21.9±	> 100	72.0±	57.6±	19.1±	> 100	75.6±	90.3±
6	20.6	> 100	8.7	11.8	2.9	> 100	53.7	11.0
6	> 100	> 100	> 100	> 100	> 100	> 100	> 100	> 100

Conclusions

Here presented novel modification of phenanthridine exocyclic amines by introduction of biguanides at 3- (mono-biguanide **5**) or 3,8 (bis-biguanide **6**) position significantly influenced DNA/RNA binding properties of phenanthridine moiety. Both compounds revealed significantly higher affinity toward ds-polynucleotides in comparison to previously

studied alkylamine- (7, 8) and urea-analogues (9), which clearly points to the significant contribution of biguanide substituents in DNA/RNA binding. Closer examination of previously studied bis-guanidinium derivatives of ethidium bromide pointed out that as small structural difference as permanently charged heterocyclic nitrogen can have a profound effect on DNA/RNA binding; whereby charged derivative is classical DNA intercalator⁵, while neutral derivative (DB950)¹³ showed DNA sequence-dependent binding modes. Structurally more similar to latter, neutral derivative of ethidium (DB950),¹³ **5** and **6** also switch binding mode from intercalation into dGdC-DNA to minor groove binding to dAdT-DNA. Consequently, both compounds were able (especially bis-biguanide **6**) to distinguish by YES-NO answer in two highly sensitive spectroscopic methods between dGdC (fluorescence quenching, negative ICD band) and dAdT (fluorescence increase, positive ICD band). All spectrophotometric changes take place at submicromolar concentrations due to the exceptionally high affinity of **5** and **6** toward ds-DNA. Moreover, here presented results show that further increase of a molecule length (**6** is longer than DB950¹³) and introduction of additional hydrogen-bonding possibilities within DNA minor groove (biguanide can form more H-bonds than guanidine) didn't abolish intercalation of **6** into dGdC.

Moreover, **5** and **6** retained a capacity to intercalate into ds-RNA, thus being promising structures to test against RNA target, the HIV-1 Rev Response Element (RRE), in line with profoundly modulated affinity and selectivity of ethidium-urea, pyrrole, or guanidinium derivatives.⁵

Such a switching of DNA/RNA binding mode is not a common property of small molecules,^{3,13} and usually it is associated with profound effects on biological activity and/or selective spectroscopic properties of complexes formed. Furthermore, specific vibrational bands of guanidine moiety allowed more detailed structural investigation of DNA complexes formed at biologically relevant conditions (10-50 micromolar concentrations) by application of SERS spectroscopy, rather novel technique in DNA/RNA studies.

The binding results of **5** and **6** to ds-DNA and ds-RNA indicated that pH of a solution and structure of both, polynucleotide and compound, have a great influence on the formation of a complex. At pH 5.0 due to the protonation of heterocyclic nitrogen, both compounds induced higher stabilization effects on polynucleotides and exhibited stronger changes in CD spectra than at pH 7.0. Advantages of a pH-controlled DNA/RNA binding combined with selective spectrophotometric signalling could be employed in numerous biochemical studies, for instance solid tumours have significantly lowered extracellular pH⁵⁶ and several antitumour drugs owe their preferential accumulation in tumour tissue due to weakly acidic pKa value⁵⁵. Although low *in vitro* cytotoxicity of both compounds against human cell lines abolishes their application as antitumour drugs, just the same makes them interesting lead compounds for a development of novel low-toxic spectrophotometric probes.

Future prospects in study of biguanide-phenanthridine derivatives associated to extended length and increased

hydrogen-bonding possibility of **5** and **6** will be also related to interactions with triplex and quadruplex DNA and DNA/RNA constructs. Namely, recently was reported increased affinity of extended ethidium bromide derivative toward triple helices;⁵⁷ as well as selective interactions of closely related ethidium derivatives with various G-quadruplex DNA.⁵⁸

Experimental

Synthetic procedures

Synthesis of 1-(6-methylphenanthridin-8-yl)biguanide · 2HCl (**5**).

To a solution of 8-amino-6-methylphenanthridine (**3**; 0.19 g, 0.91 mmol) and 3M hydrochloric acid (304 μ l, 0.033 g, 0.91 mmol) was added dicyandiamide (0.0774 g, 0.91 mmol). The resulting suspension was stirred at 90°-100°C for 3-4 hours. The reaction mixture was then dissolved in methanol, filtered off and dried. After recrystallization from methanol, the product was obtained as a yellow solid (0.178 g, 59.3%). M.p. = 275-277°C; ¹H-NMR

(DMSO-*d*₆) δ / ppm: 3.04 (s, phen-CH₃, 3H), 7.07 (brs, NH₂, 2H), 7.35 (brs, NH=C-NH-C=NH, 3H), 7.70 – 7.75 (m, phen-H₂, phen-H₃, 2H), 8.01 (d, phen-H₉, 1H, J₉₋₁₀ = 8.88 Hz), 8.16 (d, phen-H₄, 1H, J₃₋₄ = 7.86 Hz), 8.43 (s, phen-H₇, 1H), 8.68 (d, phen-H₁, 1H, J₁₋₂ = 7.86 Hz), 8.77 (d, phen-H₁₀, 2H, J₉₋₁₀ = 8.94 Hz), 10.24 (s, NH, 1H); ¹³C-NMR (DMSO-*d*₆) δ / ppm: 22.46(phen-CH₃), 116.32 (phen-H₇), 122.33 (phen-H₁), 123.28, 123.47 (phen-H₁₀), 125.64, 125.89, 126.38, 126.84 and 128.30 (phen-H₂ and phen-H₂), 127.74, 138.47, 154.89, 158.33, 159.03, 161.34; IR (KBr) ν (cm⁻¹): 619, 766, 851, 874, 1041, 1155, 1221, 1242, 1340, 1365, 1404, 1487, 1508, 1519, 1560, 1637, 1651, 1917, 2345, 2630, 3024, 3082, 3178, 3292, 3363; ES-MS *m/z* for C₁₆H₁₆N₆ (*M_r*=292.35 gmol⁻¹) 293.147 [M+H]⁺; HRMS (MALDI / TOF) for C₁₆H₁₆N₆ [M+H]⁺ *M_r* calcd = 293.1509; *M_r* found = 293.1520.

Synthesis of 1-(6-methylphenanthridine-3,8-diyl)dibiguanide · 3HCl (**6**)

To a solution of 3,8-diamino-6-methylphenanthridine (**4**; 0.15 g, 0.67 mmol) and 3M hydrochloric acid (480 μ l, 0.049 g, 1.345 mmol) was added dicyandiamide (0.113 g, 1.345 mmol). The resulting suspension was stirred at 90°-100°C for 3-4 hours. The reaction mixture was then dissolved in methanol and filtered off to give a light brown solid (0.147 g, 47%). The product was further purified by dissolving in water (10 ml) and treating with DOWEX(R) 1 X 2, Cl(-)-form ion exchange resin at room temperature. It was then filtered over an activated Varian's 'Bondelut' Mega Be-C18 column (activated with 10 ml methanol, 10 ml water), the remainder was eluted from the column using 2% methanol / water and evaporated to 0.12 g of a brown solid (38.5%). M.p. = >320°C; ¹H-NMR (DMSO-*d*₆) δ / ppm: 2.81 (s, phen-CH₃, 3H), 7.12 (brs, NH₂, 2H), 7.19 (brs, NH₂, 2H), 7.40 (brs, NH=C-NH-C=NH, 6H), 7.53 (d, phen-H₂, 1H, J₁₋₂ = 7.92 Hz), 7.80 (d, phen-H₉, 1H, J₉₋₁₀ = 7.62 Hz), 8.03 and 8.25 (s, phen-H₄, phen-H₇, 2H), 8.49 (d, phen-H₁, 1H, J₁₋₂ = 8.88 Hz), 8.59 (d, phen-H₁₀, 1H, J₉₋₁₀ = 9.18 Hz), 10.22 and 10.30 (s, NH, 2H); ¹³C-NMR (DMSO-*d*₆) δ / ppm: 22.91 (phen-CH₃), 116.10 and 118.32 (phen-H₇, phen-H₄), 118.85, 120.06 (phen-H₂), 122.56 (phen-H₁), 122.97 (phen-H₁₀), 124.78

(phen-H9), 125.10, 127.67, 137.68, 138.71, 154.93, 155.08, 158.48, 161.29, 161.40, 162.73; IR (KBr) ν (cm⁻¹): 602, 669, 825, 1005, 1116, 1138, 1396, 1489, 1541, 1564, 1624, 1653, 1743, 2343, 2360, 2924, 3215, 3404; ES-MS m/z for C₁₈H₂₁N₁₁ ($M_r=391.44$ g mol⁻¹) 392.212 [M+H]⁺, 196.614 [M+2H]²⁺; HRMS (MALDI / TOF) for C₁₈H₂₁N₁₁ [M+H]⁺ M_r calcd = 392.2054; M_r found= 392.2051.

Materials and methods

¹H NMR and ¹³C NMR spectra were recorded on a Bruker AV300 or Bruker AV600 (at 300 and 600 MHz) at 25°C. Chemical shifts (δ) were given in parts per million (ppm) relative to tetramethylsilane as an internal standard and coupling constants (J) in hertz. The splitting patterns in the ¹H NMR spectra are denoted as follows: s (singlet), brs (broad singlet), d (doublet), t (triplet), m (multiplet). Melting points were determined on a Kofler melting points apparatus and are uncorrected. Infrared spectra were recorded on a BOMEM MB 102 spectrophotometer and spectral bands are expressed in 'wave numbers' with the unit cm⁻¹. Mass spectra were obtained using BRUKER micrOTOF spectrometer and Waters Micromass ZQ. The pH measurement was carried out using Mettler TOLEDO MP220 pH meter calibrated with commercially available buffered aqueous solutions of pH standards 4.00 and 7.00. The UV/vis spectra were recorded on a Varian Cary 100 Bio spectrophotometer, CD spectra on JASCO J815 spectrophotometer and fluorescence spectra on a Varian Cary Eclipse spectrophotometer at 25°C using appropriate 1 cm path quartz cuvettes. For study of interactions with DNA and RNA, aqueous solutions of compounds buffered to pH 5.0 (citric acid/NaOH buffer, $I=0.03$ mol dm⁻³) and pH 7.0 (buffer sodium cacodylate, $I=0.05$ mol dm⁻³) were used.

Relative fluorescence quantum yields (Q) were determined by the standard procedure⁵⁹. All samples were purged with argon to displace oxygen, and emission spectra were recorded from 350–600 nm and corrected for the effects of time- and wavelength-dependent light-source fluctuations by use of a rhodamine 101 standard, a diffuser and the software provided with the instrument. As the standard we used 1-N-acetyltryptophanamide (NATA, Fluka, Buchs, Switzerland) with published fluorescence quantum yield $Q=0.14$.⁶⁰ The NATA concentration in fluorescence measurements had an optical absorbance below 0.05 at the excitation wavelength while **5** and **6** had optical absorbencies between 0.06 and 0.15 at the excitation wavelength.

Polynucleotides were purchased as noted: poly rA–poly rU, poly dG–poly dC, poly dA–poly dT, poly(dAdT)₂ (Sigma), calf thymus (ct)-DNA (Aldrich). Polynucleotides were dissolved in Na-cacodylate buffer, $I=0.05$ mol dm⁻³, pH 7.0. The calf thymus ctDNA was additionally sonicated and filtered through a 0.45 mm filter.⁶¹ Polynucleotide concentration was determined spectroscopically as the concentration of phosphates. Spectrophotometric titrations were performed at pH 5.0 ($I=0.03$ mol dm⁻³, citric acid/NaOH buffer) and pH 7.0 ($I=0.05$ mol dm⁻³, buffer sodium cacodylate) by adding portions of polynucleotide solution into the solution of the studied compound for UV/vis and

fluorimetric experiments and for CD experiments were done by adding portions of compound stock solution into the solution of polynucleotide. In fluorimetric experiments excitation wavelength of $\lambda_{exc} \geq 300$ nm was used to avoid the inner filter effect caused due to increasing absorbance of the polynucleotide. Emission was collected in the range $\lambda_{em}=380$ –600 nm. Processing titration data by means of Scatchard equation³² gave values of ratio $n=0.1 \pm 0.05$. Values for K_s given in Table 3 all have satisfactory correlation coefficients (>0.99). Thermal melting curves for DNA, RNA and their complexes with studied compounds were determined as previously described^{29,38} by following the absorption change at 260 nm as a function of temperature. Absorbance of the ligands was subtracted from every curve and the absorbance scale was normalized. T_m values are the midpoints of the transition curves determined from the maximum of the first derivative and checked graphically by the tangent method.²⁹ The ΔT_m values were calculated subtracting T_m of the free nucleic acid from T_m of the complex. Every ΔT_m value here reported was the average of at least two measurements. The error in ΔT_m is $\pm 0.5^\circ\text{C}$.

Viscometry measurements were conducted with an Ubbelohde viscometer system AVS 370 (Schott). The temperature was maintained at 25 \pm 0.1 °C. Aliquots of drug stock solutions were added to 2.5 ml of 5×10^{-4} mol dm⁻³ polynucleotide solution in buffer sodium cacodylate, $I = 0.05$ mol dm⁻³, pH 7.0, with a compound to polynucleotide phosphate ratio r less than 0.2. Dilution never exceeded 4% and was corrected for in the calculations. The flow times were measured at least five times optically with a deviation of ± 0.2 s. The viscosity index α was obtained from the flow times at varying r according to the following equation:⁶²

$$L/L_0 = [(t_r - t_0) / (t_{\text{polynucleotide}} - t_0)]^{1/3} = 1 + \alpha \cdot r$$

Where t_0 , $t_{\text{polynucleotide}}$ and t_r denote the flow times of buffer, free polynucleotide and polynucleotide complex at ratio $r_{[\text{compound}] / [\text{polynucleotide}]}$, respectively; L/L_0 is the relative DNA/RNA lengthening. The L/L_0 to $r_{[\text{compound}] / [\text{polynucleotide}]}$ plot was fitted to a straight line that gave slope α . The error in α is < 0.1 .

SERS spectroscopy

Chemicals: Silver nitrate (Kemika) and trisodium citrate (Kemika) were of analytical reagent grade and used as supplied for the silver colloid preparation. Water was purified by passage through Milli-Q (Millipore) deionizing and filtration columns. Cacodylate buffer contained 0.05 mol dm⁻³ sodium cacodylate adjusted to pH 7.0 by 0.1 mol dm⁻³ HCl.

Colloid preparation: Before preparation of colloid all glassware was thoroughly cleaned with a detergent solution, followed by treatment in 5 % nitric acid, and finally rinsed with water of Milli-Q purity. Silver colloid was prepared according to a modified Lee and Meisel reduction method with citrate.^{63,64} Silver nitrate (18 mg) was suspended in water (100 mL) and heated rapidly to boiling under stirring. A 1 % (w/v) trisodium citrate aqueous solution (2 mL) was added to the boiling solution and kept boiling gently for 90 min with continuous stirring. The resulting colloidal solution was

greenish yellow with the maximum at 424 nm in the UV/Vis absorption spectrum. pH value of the prepared colloid was 6.9.

Samples preparation: SERS spectra of the biguanide species were measured in the silver citrate colloid. Samples with ctDNA were prepared by mixing the silver citrate colloid (425 μL), the **5** or **6** stock solution (50 μL , $c = 5 \times 10^{-4} \text{ mol dm}^{-3}$) and ctDNA (25 μL , $c = 2 \times 10^{-2} \text{ mol dm}^{-3}$). The resulting [5,6]/[phosphate] ratio was 1/20. To study the effect of the cacodylate buffer on the biguanide SERS spectra, samples were prepared in the same way but adding the buffer solution instead of the nucleic acid. In all working samples the final concentration of the biguanide species was $5 \times 10^{-5} \text{ mol dm}^{-3}$.

Instrumentation: FT-Raman and SERS spectra were measured on a Bruker Equinox 55 interferometer equipped with a FRA 106/S Raman module using Nd-YAG laser excitation at 1064 nm and a laser power of 500 mW. Raman spectra were taken in the 3500–100 cm^{-1} range. To obtain good spectral definition, 128 scans at a spectral resolution of 4 cm^{-1} were averaged for each spectrum. UV/Vis absorption measurement of the silver citrate colloid was carried out with an Analytik Jena spectrometer (model SPECORD 200). Conventional quartz cells (10 mm \times 10 mm) were used throughout. For pH measurements, a Mettler Toledo pH meter (model MP 220) with a Mettler Toledo InLab@413 combined glass-calomel electrode was used. The pH meter was calibrated with standard aqueous buffer solutions of pH 7.00 and 4.01.

Cell cultures and MTT assay

Cell culturing: Human tumour cell lines, stomach epithelial gastric adenocarcinoma (AGS), pancreatic carcinoma (MiaPaCa2), colon adenocarcinoma (CaCo-2), larynx carcinoma (HEp-2), cervix adenocarcinoma (HeLa), bronchoalveolar carcinoma (NCI-H358), normal human foreskin cell line (BJ) fibroblast morphology between 27-29 passages and Madine-Darby canine kidney (MDCK) cells between 24-26 passages, were cultured in tissue culture flasks (25.75 cm^2) and grown as monolayer's. Cells were cultured in Dulbecco's modified Eagle medium – DMEM (Gibco, EU) supplemented with 10% heat-inactivated foetal bovine serum (FBS, Gibco, EU), 2mM glutamine, and 100U/0.1mg penicillin/streptomycin. AGS and NCI-H358 cell lines were cultivated in RPMI 1640 (Gibco, EU) medium supplemented with 10% heat-inactivated foetal bovine serum (FBS, Gibco, EU), 2 mmol dm^{-3} glutamine, 1mmol dm^{-3} sodium pyruvate, 10 mmol dm^{-3} HEPES and 100U/0.1 mg penicillin/streptomycin. To detach from flask surface, cells were trypsinized using 0.25% trypsin/EDTA solution. Cells were culture in humidified atmosphere under the condition of 37°C/5% of CO_2 gas in the CO_2 incubator (Shell Lab, Sheldon Manufacturing, USA).

Cytotoxicity evaluation by MTT assay:⁶⁵ Tested compounds (**5**, **6**) were prepared as stock solutions ($5 \times 10^{-3} \text{ mol dm}^{-3}$) in high pure water with addition of 5.2% of 0.1 mol dm^{-3} HCl (**5**) and 4.9% of 0.1 mol dm^{-3} HCl (**6**). Influence of added HCl was evaluated through the percentage range like it was in the range of tested substances. Addition of HCl in solutions had no effect on their ability to suppress cell growth. Working solutions ($10^{-3} - 10^{-6} \text{ mol dm}^{-3}$) were prepared prior to testing. Cytotoxic

effects were determined by MTT assay. Cells were seeded in 96 micro well flat bottom plates (Greiner, Frickenhausen, Austria) at concentration 2×10^4 cells/mL and left overnight in the CO_2 incubator allowing them to attach to the plate surface. 72 h after compound addition growth medium was discarded and 5mg/mL of MTT was added. After 4h incubation at 37°C water insoluble MTT-formazan crystals were dissolved in DMSO. Plates were shaken at high speed to ensure total dissolution of crystals which is pre request for absorbance measuring. Absorbance was measured at 570 nm on Elisa micro plate reader (Stat fax 2100, Pharmacia Biotech, Uppsala, Sweden). Control, none treated, cells were grown under the same conditions. All experiments were performed at least three times in triplicates. The IC_{50} , a compound concentration which reduced cellular viability by 50% compared to the viability of control cells after 72 h of treatment, were determined by constructing a dose-response curve and used as a parameter to compare cytotoxicity among tested compounds. STATISTIC 7 software and Kolmogorov – Smirnov two sample test were used to statistically evaluate data obtained from MTT test.

Acknowledgments: The authors are grateful for a financial support of this study by the Ministry of Science, Education and Sport of Croatia (Projects 098-0982914-2918, 119-1191342-2959, 219-0982914-2176; 219-0982914-2179).

Notes and references

^a Division of Organic Chemistry and Biochemistry, Ruder Bošković Institute, Bijenička cesta 54, PO Box 180, HR-10002 Zagreb, Croatia. E-mail: pianta@irb.hr

^b Laboratory of Analytical Chemistry, Department of Chemistry, Faculty of Science, University of Zagreb, Horvatovac 102a, HR-10000 Zagreb, Croatia.

^c Department of Medicinal Chemistry and Biochemistry, School of Medicine, J.J. Strossmayer University of Osijek, 31000 Osijek, Croatia

^d Clinical Institute of Nuclear Medicine and Radiation Protection, University Hospital Centre Osijek, 31000 Osijek, Croatia

† Electronic Supplementary Information (ESI) available: [detailed CD experiments, viscometry, Table with assignment of SERS data, additional biological data]. See DOI: 10.1039/b000000x/

¹ N. T. Thuong, C. Hélène, *Angew. Chem. Int. Ed. Engl.*, 1993, **32**, 666.

² E. Trinquet, G. Mathis, *Mol. Bio. Syst.*, 2006, **2**, 380.

³ M. Demeunynck, C. Bailly and W. D. Wilson, *DNA and RNA Binders*, Wiley-VCH: Weinheim, 2002.

⁴ N. W. Luedtke, Q. Liu and Y. Tor, *Chem. Eur. J.*, 2005, **11**, 495.

⁵ N. W. Luedtke, Q. Liu and Y. Tor, *Bioorg. Med. Chem.*, 2003, **11**, 5235.

⁶ a) T. Kubar, M. Hanus, F. Ryjacek and P. Hobza, *Chem. Eur. J.*, 2006, **12**, 280; b) J. Duhamel, J. Kanyo, G. Dintergottlieb and P. Lu, *Biochemistry*, 1996, **35**, 16 687; c) S. A. Winkle, L. S. Rosenberg and T. R. Krugh, *Nucleic Acids Res.*, 1982, **10**, 8211.

⁷ N. Stevens, N. O'Connor, H. Vishwasrao, D. Samaroo, E. R. Kandel, D. L. Akins, C. M. Drain and N. J. Turro, *J. Am. Chem Soc.*, 2008, **130**, 7182.

⁸ L. W. Yielding and W. J. Firth III, *Mutation Research*, 1980, **71**, 161; M. Fukunaga, B. A. Cox, R. S.von Sprecken and L. W. Yielding, *Mutation Research*, 1984, **127**, 31.

⁹ M. Maiti and G. S. Kumar, *Med. Res. Rev.*, 2007, **27**,649.

¹⁰ a) A. D. C. Parenty, L. V. Smith, K. M. Guthrie, D.-L. Long, J. Plumb, R. Brown and L. Cronin, *J. Med. Chem.*, 2005, **48**, 4504. b) I. Kock, D. Heber, M. Weide, U. Wolschendorf and B. Clement, *J. Med. Chem.*, 2005, **48**, 2772.

- ¹¹ W. G. Lewis, L. G. Green, F. Grynszpan, Z. Radić, P. R. Carlier, P. Taylor, M. G. Finn and K. B. Sharpless, *Angew. Chem. Int. Ed.*, 2002, **41**, 1053.
- ¹² A. Krasinski, Z. Radić, R. Manetsch, J. Rauschel, P. Taylor, K. B. Sharpless and H. C. Kolb, *J. Am. Chem. Soc.*, 2005, **127**, 6686.
- ¹³ C. Bailly, R. K. Arafa, F. A. Tanious, W. Laine, C. Tardy, A. Lansiaux, P. Colson, D. W. Boykin and W. D. Wilson, *Biochemistry*, 2005, **44**, 1941.
- ¹⁴ K. Ohara, M. Smietana, A. Restouin, S. Mollard, J. P. Borg, Y. Collette and J. J. Vasseur, *J. Med. Chem.*, 2007, **50**, 6465.
- ¹⁵ G. Malojčić, I. Piantanida, M. Marinić, M. Žinić, M. Marjanović, M. Kralj, K. Pavelić and H.-J. Schneider, *Org. Biomol. Chem.*, 2005, **3**, 4373.
- ¹⁶ a) M. Radić Stojković and I. Piantanida, *Tetrahedron*, 2008, **64**, 7807. b) M. Radić Stojković, S. Marzi, Lj. Glavaš-Obrovac and I. Piantanida, *Eur. J. Med. Chem.*, 2010, **45**, 3281.
- ¹⁷ I. Juranović, Z. Meić, I. Piantanida, L.-M. Tumor and M. Žinić, *J. Chem. Soc., Chem. Commun.*, 2002, 1432.
- ¹⁸ L.-M. Tumor, I. Piantanida, I. Juranović, Z. Meić, S. Tomić and M. Žinić, *J. Chem. Soc., Chem. Commun.*, 2005, 2561.
- ¹⁹ L. Hernandez-Folgado, D. Baretić, I. Piantanida, M. Marjanović, M. Kralj, T. Rehm and C. Schmuck, *Chem. Eur. J.*, 2010, **16**, 3036.
- ²⁰ a) F. H. S. Curd and F. L. Rose, *J. Chem. Soc.*, 1946, 729. b) M. Angelo, D. Ortwine, D. Worth, L. M. Werbel and J. W. McCall, *J. Med. Chem.*, 1983, **26**, 1258.
- ²¹ a) P. Rây, *Chem. Rev.*, 1961, **61**, 313; b) A. Syamal, *J. Sci. Ind. Res.*, 1978, **37**, 661.
- ²² a) T. Ikeda, H. Yamaguchi and S. Tazuke, *Antimicrobial Agents and Chemotherapy*, 1984, **26**, 139; b) S. Mayer, D. M. Daigle, E. D. Brown, J. Khatri and M. G. Organ, *Journal of Combinatorial Chemistry*, 2004, **6**, 776; c) G. T. Wernert, D. A. Winkler, B. C. Elmes and G. Holan, *Australian Journal of Chemistry*, 2004, **57**, 77.
- ²³ S. Bag, N. R. Tawari, R. Sharma, K. Goswami, M. V. R. Reddy and M. S. Degani, *Acta Tropica*, 2010, **113**, 48.
- ²⁴ S. Bastaki, *Int J Diabetes & Metabolism*, 2005, **13**, 111.
- ²⁵ a) L. M. Bernstein, *Cancer Letters*, 2005, **224**, 203; b) A. Vazquez-Martin, C. Oliveras-Ferraros, S. del Barco, B. Martin-Castillo and J. A. Menendez *Ann Oncol*, 2009, **20**, 592.
- ²⁶ S. L. Shapiro, V. A. Parrino, E. Rogow and L. Freedman, *J. Am. Chem. Soc.*, 1959, **81**, 3725.
- ²⁷ G. T. Morgan and L. P. Walls, *J. Chem. Soc.*, 1931, 2447.
- ²⁸ S. R. Ernst, *Acta Cryst.*, 1977, **B33**, 237.
- ²⁹ I. Piantanida, B. S. Palm, M. Žinić and H. J. Schneider, *J. Chem. Soc., Perkin Trans. 2*, 2001, 1808.
- ³⁰ J. Ramstein, M. Leng, *Biochim. Biophys. Acta*, 1972, **281**, 18. b) M. G. Badea and S. Georghiou, *Photochem. and Photobiol.*, 1976, **24**, 417; c) S. Georghiou, *Photochem. and Photobiol.*, 1977, **26**, 59.
- ³¹ a) S. O. Kelley and J. K. Barton, *Science*, 1999, **283**, 375; b) S. A. E. Marras, F. R. Kramer, S. Tyagi, *Nucleic Acids Res.*, 2002, **30**, 122.
- ³² G. Scatchard, *Ann. N.Y. Acad. Sci.*, 1949, **51**, 660.; J. D. McGhee, P. H. von Hippel, *J. Mol. Biol.*, 1976, **103**, 679.
- ³³ N. Berova, K. Nakanishi and R. W. Woody, *Circular Dichroism Principles and Applications*; Wiley-VCH: New York, NY, 2nd edn, 2000.
- ³⁴ A. Rodger and B. Norden, *Circular Dichroism and Linear Dichroism*; Oxford University Press: New York, 1997.
- ³⁵ M. Eriksson and B. Nordén, *Methods in Enzymology*, 2001, **340**, 68.
- ³⁶ S. Neidle, *Nat Prod Rep.*, 2001, **18**, 291.
- ³⁷ C. Bailly, P. Colson, C. Houssier and F. Hamy, *Nucl. Acids Res.*, 1996, **24**, 1460.
- ³⁸ J. L. Mergny, L. Lacroix, *Oligonucleotides*, 2003, **13**, 515.
- ³⁹ C. R. Cantor, P. R. Schimmel, *Biophysical Chemistry*; WH Freeman: San Francisco, CA, 1980, 1109.
- ⁴⁰ L. P. G. Wakelin, *Med. Res. Rev.*, 1986, **6**, 277.
- ⁴¹ H. Morjani, J.-F. Riou, I. Nabiev, F. Lavelle and M. Manfait, *Cancer Res*, 1993, **53**, 4784.
- ⁴² I. Nabiev, I. Chourpa and M. Manfait, *J. Phys. Chem.*, 1994, **98**, 1344.
- ⁴³ I. Nabiev, A. Baranov, I. Chourpa, A. Beljebbar, G. D. Sockalingum and M. Manfait, *J. Phys. Chem.*, 1995, **99**, 1608.
- ⁴⁴ G. Breuzard, J.-M. Millot, J.-F. Riou and M. Manfait, *Anal. Chem.*, 2003, **75**, 4305.
- ⁴⁵ A. Ianoul, F. Fleury, O. Duval, R. Waigh, J.-C. Jardillier, A. J. P. Alix and I. Nabiev, *J. Phys. Chem. B*, 1999, **103**, 2008.
- ⁴⁶ C.-Y. Wu, W.-Y. Lo, C.-R. Chiu and T.-S. Yang, *J. Raman Spectrosc.*, 2006, **37**, 799.
- ⁴⁷ F. R. Dollish, W. G. Fateley and F. F. Bentley, *Characteristic Raman Frequencies of Organic Compounds*, John Wiley & Sons, New York, 1974.
- ⁴⁸ P. Sett, M. Ghosh, P. K. Mallick and J. Chowdhury, *J. Raman Spectrosc.*, 2008, **39**, 1878.
- ⁴⁹ I. Matulková, I. Němec, I. Císařová, P. Němec and Z. Mička, *J. Mol. Struct.*, 2008, **886**, 103.
- ⁵⁰ I. Matulková, I. Němec, I. Císařová, P. Němec and P. Vaněk, *J. Mol. Struct.*, 2010, **966**, 23.
- ⁵¹ G. Weng, C. X. Chen, V. Balogh-Nair, R. Callender and D. Manor, *Protein Sci.*, 1994, **3**, 22.
- ⁵² a) E. C. Long and K. Barton, *Acc. Chem. Res.*, 1990, **23**, 271; b) G. Dougherty and J. R. Pilbrow, *Int. J. Biochem.*, 1984, **16**, 1179; c) M. K. Pall and J. K. Ghosh, *Spectrochimica Acta*, 1995, **51**, 489.
- ⁵³ J. W. Locasale and L. C. Cantley, *BMC Biology*, 2010, **8**, 88.
- ⁵⁴ V. Rausch, L. Liu, G. Kallifatidis, B. Baumann, J. Mattern, J. Gladkikh, T. Wirth, P. Schemmer, M. W. Buchler, M. Zoller, A. V. Salnikov and I. Herr, *Cancer Res.*, 2010, **70**, 5004.
- ⁵⁵ N. Raghunand, R. J. Gillies, *Drug Resistance Updates*, 2000, **3**, 39.
- ⁵⁶ P. Wong, C. Lee and I. F. Tannock, *Clin Cancer Res.*, 2005, **11**, 3553; R. J. Gillies, I. Robey and R. A. Gatenby, *J. Nucl. Med.*, 2008, **49**, 24.
- ⁵⁷ V. K. Tam, Q. Liu, Y. Tor, *Chem. Commun.*, 2006, 2684.
- ⁵⁸ a) F. Rosu, E. De Pauw, L. Guittat, P. Alberti, L. Lacroix, P. Mailliet, J. F. Riou and J. L. Mergny, *Biochemistry*, 2003, **42**, 10361.; b) F. Koepfel, J. F. Riou, A. Laoui, P. Mailliet, P. B. Arimondo, D. Labit, O. Petitgenet, C. Helene and J. L. Mergny, *Nucleic Acids Res*, 2001, **29**, 1087-1096.
- ⁵⁹ J. N. Miller, *Standards for Fluorescence Spectrometry*, Chapman and Hall, London, 1981.
- ⁶⁰ M. R. Eftink, Y. Jia, D. Hu and C. A. Ghiron, *J. Phys. Chem.*, 1995, **99**, 5713.
- ⁶¹ J. B. Chaires, N. Dattagupta and D. M. Crothers, *Biochemistry*, 1982, **21**, 3933.
- ⁶² G. Cohen and H. Eisenberg, *Biopolymers*, 1969, **8**, 45; M. Wirth, O. Bucharadt, T. Koch, P. E. Nielsen and B. Nordén, *J. Am. Chem. Soc.*, 1988, **110**, 932.
- ⁶³ P. C. Lee and D. Meisel, *J. Phys. Chem.*, 1982, **86**, 3391.
- ⁶⁴ C. H. Munro, W. E. Smith, M. Garner, J. Clarkson and P. C. White, *Langmuir*, 1995, **11**, 3712.
- ⁶⁵ G. Mickisch, S. Fajta, H. Bier, R. Tschada and P. Alken, *Urol. Res.*, 1991, **19**, 99.